A simple model to predict the thermal performance of a ventilated facade with phase change materials

Alvaro de Gracia[1], Albert Castell[1], Cèsar Fernández[2], Luisa F. Cabeza[1*]

[1*] GREA Innovació Concurrent, Universitat de Lleida, Edifici CREA, Pere de Cabrera s/n, 25001, Lleida, Spain. Tel: +34.973.00.35.77. Email: lcabeza@diei.udl.cat
[2] Computer Sciences Department, University of Lleida

Abstract

Appropriate design and control strategies are crucial for the implementation of certain complex active systems in the building sector. Suitable and user-friendly numerical tools have to be available to architects and engineers, so they can incorporate innovative active systems in their building designs. The thermal response of a ventilated facade with phase change material in its air chamber for cooling applications is studied in this paper. The system makes use of low temperatures at night to solidify the phase change material, and store it solid for a later cooling supply to the interior of the building. This active technology is very sensitive to the weather conditions as well as to the defined operational schedule (charge, storage and discharge periods definition). Two different numerical approaches have been developed to better understand this system and to define different control strategies, as well as to determine their potential to reduce the energy consumption in the building for cooling purposes. First, a finite control volume approach was applied to describe the ventilated facade with latent heat storage. The important computational cost and complexity of this numerical methodology leaded the authors to develop a simple numerical model based on the assumption that the exchange between the air and phase change material inside the ventilated facade occurs at isothermal conditions. Both models were validated against experimental data, and even though the isothermal model presented slightly higher deviation from the experimental results than the finite control volume one, it is presented as a suitable numerical tool for architects and engineers because of its light computational cost and versatility.

Key words

Phase change materials (PCM), Thermal energy storage (TES), Numerical modeling, Buildings

1. Introduction

It is well known that the high energy demand of HVAC (Heat, Ventilated and Air Conditioned) systems used in the building sector and its reduction is considered a key aspect in energy, economical and sustainable point of view. Numerous energy policies have been recently implemented worldwide to achieve this goal, such as the European directive 2010/31/EU [1]. According to the ETP 2012 [2], the building sector consumes approximately 32% of global final energy use, making it responsible for almost 15% of total direct energy-related CO_2 emissions from final energy consumers. Several studies showed that thermal energy storage (TES) systems can be efficiently applied in building design as passive or active systems to reduce the energy required by HVAC systems [3-5].

Within this context, the incorporation of latent heat thermal energy storage (LHTES) systems based on the use of phase change materials (PCM) in both passive and active buildings systems [6,7] has been a big topic of interest because of the high energy density that these materials can provide. However, these technologies have to overcome some important barriers before being widely implemented in the building sector. Apart from the economics, one of the main important technical barriers is the complexity of these systems to be implemented in the building design [8]. In order to better understand and optimize the design of these systems, the use of numerical tools is required. Even though several numerical models are available in the literature (both for passive [9,10] and active [11,12] systems), they are developed for specific applications, are non-user-friendly, and require high computational costs as well as very specific knowledge of the numerical models. These drawbacks strongly limit their use in the building sector and hence, discard the possible implementation of LHTES systems in the building design.

In this paper, a simple numerical tool is developed and presented to describe the performance of a ventilated facade with PCM panels in its air chamber for cooling purposes. The simple tool (isothermal model from here on) is based on the assumption that the heat exchange process between the air flowing through the ventilated facade cavity and the PCM panels occurs in isothermal conditions. Even though the model is

here presented for such specific application, it can be easily adaptable to any active system containing air-PCM heat exchange.

The isothermal model is compared against a finite control volume approach (control volume model from here on) and both numerical models are validated against experimental measurements. Moreover, some key aspects, such as the treatment of the inlet temperature in the active system, are also discussed.

2. Methodology

2.1 Description of the system

A versatile ventilated double skin facade (VDSF) with PCM panels in its air channel was tested experimentally to provide energy benefits both for heating [13] and cooling [14]. Figure 1 shows the prototype tested in the experimental set-up located in Puigverd de Lleida (Spain).

In the air cavity between the two skins of the VDSF, 112 PCM panels (RT21 macro-encapsulated CSM panels from Rubitherm Technologies GmbH [15]) are installed creating 14 channels, as it can be seen in Figure 2. Six automatized gates were installed at the different openings of the channel in order to control the operational mode of the facade. Moreover, three fans with variable power output (ranging between 17 W and 120 W each) were placed at the inlet of the air channel to provide mechanical ventilation when needed.

The ventilated facade operates as a cold storage system, since it uses the low temperature at night to solidify the PCM. During the peak load hours, when there is a cooling demand, the air is cooled down by the PCM providing a cooling supply. The operational principle of the system is summarized in Figure 3. The cold storage sequence is based on a charge process (Figure 3a), a storage period (Figure 3b), and a cooling discharge (Figure 3c). It is important to notice that both charge and discharge processes are driven by mechanical ventilation; hence, an appropriate control strategy is mandatory for the use of this system in order to ensure that the electrical energy

consumption by the fans is minimized and net energy benefits can be achieved. Within this context, the necessity of a simple and computationally light numerical tool is reaffirmed, since such a tool could be implemented in any basic control system at building scale or used for the development of control strategies.

A full description of the sensors used in the experimental facility is given in de Gracia et al. [13]. The sensors used for experimental validation purposes were the following:

- Indoor and outdoor air temperature (at a height of 1.5 m and 4.5 m) measured with ELEKTRONIK EE21.
- Air temperature of the cavity at different heights and locations (10 Pt-100 with an irradiative cover).
- Temperature of the PCM at three different heights (3 Thermocouples Type T, 0.5 mm thick inserted in the PCM panels).
- Horizontal and vertical global solar radiation measured with two Middleton Solar pyranometers SK08.

Saelens et al. [16] reported significant differences between the inlet air temperature of the facade and the indoor and outdoor temperatures (usually known and used for design and control). These differences were also observed in the experiments performed in this research during the validation of the models. However, both the control volume model and the isothermal model use the indoor and outdoor temperature during the simulation. Therefore, in order to estimate the error provided by this assumption, two control volume methods were compared. In the first method (CV1), the experimentally measured inlet temperature was introduced in the model as inlet, while in the second one (CV2), the measured outdoor and indoor temperature were set as inlet temperature in the charge and discharge processes, respectively. The isothermal model (IM) used the same boundary conditions as CV2, since they are more useful for the design procedure since inlet temperature data is not available, but weather conditions (outdoor temperature) and indoor set-point (indoor temperature) can be predicted or estimated.

2.2 Control volume model

A numerical model based on the finite control volume method [17] was developed by de Gracia et al. [18] to study the performance and to define control strategies of the same system but with less insulation in the outer skin and with PCM panels of SP22 instead of RT21. The numerical model solves the energy conservation equation during the previously defined three steps in the cold storage sequence and is based on the following assumptions:

(i) The thermal radiation between surfaces is considered one-dimensional (x).

(ii) In the CV1 model, the measured temperature at the inlet of the facade is implemented directly as a boundary condition.

(iii) In the CV2 model, the temperature of the air at the inlet of the channel is considered equal to the outer temperature during the PCM solidification period.

(iv) In the CV2 model, the temperature of the air at the inlet of the channel is considered equal to the inner temperature during the PCM melting period.

(v) The PCM is homogeneous and isotropic.

(vi) The phase change was taken into account through an equivalent heat capacity [19]. During the melting or solidification, the temperature dependence of the PCM specific heat has a triangle shape centered on T_{PCM}. This methodology was studied by Farid [20] and was found to be successful in describing the heat transfer in phase change materials.

Further details about the numerical model based on the control volume approach can be found in de Gracia et al. [18].

2.3 Isothermal model

A simple model, based on the assumption that all the PCM included in the facade is at the same temperature, was developed. The model does not require any iterative process and hence reduces dramatically the time and computational resources required in comparison to the control volume model. The model is based on the following assumptions:

(i) The air flowing through the VDSF channel during both charge and discharge process is considered as fully developed internal flow.

(ii) The temperature of the PCM is homogeneous in thickness and height of the channel. This assumption is critical for the performance of the non-iterative process and even though there will be conduction inside the material in both direction, it is justified because of the small thickness of the PCM plates (7 mm) and the forced convective nature of both charge and discharge processes.

(iii) The heat transfer coefficient is considered constant through the entire channel based on Gnielinski [21] Nusselt correlation (function of Reynolds and Prandtl).

(iv) The air only receives and releases heat from and to the PCM panels.

(v) Heat losses or gains are considered only during the storage mode of operation (when the VDSF is not charging or discharging the PCM), since both charge and discharge are driven by forced convection, which is dominant in these processes.

(vi) The manufacturer Cp vs. temperature curve of the PCM (RT21) is used [15].

The phase change is modeled as a variation of the heat capacity depending on the temperature of the PCM. A parameter called S is defined to determine how far the material is to full solidification. The value of the parameter S depends directly on the average temperature of the PCM. It has a value of 0 at the beginning of the solidification process (23ºC) and a value of 1, for fully solidified PCM at 18ºC. According to the data provided by the manufacturer [15], a latent heat of 93 kJ/kg was considered within this temperature range of phase change (from 18ºC to 23ºC). Out of this temperature range, the S value is calculated according to the ratio between the sensible heat to/from the phase change boundaries and the latent heat of the phase change range. Figure 4 presents the dependence of the heat capacity and S value with the temperature.

As it was previously said, the charge and discharge processes are assumed to behave as an internal flow through a constant temperature surface. Hence, the temperature at the outlet of the channel at an instant "n" can be calculated from the Eq.1 [22]:

$$T_{outlet}^{\ n} = T_{PCM}^{\ n} - \left(T_{PCM}^{\ n} - T_{inlet}^{\ n}\right) e^{\frac{-h \cdot A_{conv}}{\dot{m} \cdot Cp}} \qquad \text{(Eq.1)}$$

The inlet temperature (T_{inlet}^{n}) is set as the outer temperature $T_{ext}(t)$ during the solidification process and as the internal set point temperature (Tsp) of the house during the discharge process. The air heat capacity is considered constant at 1005 J/kg·K. The power of charge (Figure 3a) or discharge (Figure 3c) of the PCM can be calculated by an energy balance between the inlet and the outlet of the air flow at the "n" instant (Eq.2).

$$\dot{Q}^n = \dot{m} \cdot C_p \cdot \left(T_{out}{}^n - T_{inlet}{}^n \right) \quad \text{(Eq.2)}$$

In order to avoid any iterative method that will result in a high computational cost, the isothermal model makes use of an explicit scheme to discretize the time. Therefore, if the power of charge or discharge of the PCM is assumed to be the same during the time step between the instant "n" and the instant "n+1" the amount of energy stored or released by the PCM can be integrated through the time step (Eq.3):

$$Q_{n \to n+1} = \int_{n}^{n+1} \dot{Q}^{n} \cdot dt \quad \text{(Eq.3)}$$

Once the energy that the PCM has exchanged with the air is determined, the state of the PCM at the instant "n+1" can be calculated as expressed in Eq.4:

$$S^{n+1} = S^n + \frac{Q_{n \to n+1}}{m_{PCM} \cdot L} \quad \text{(Eq.4)}$$

The calculation of the state parameter allows determining the temperature of the PCM at the new instant of calculation "n+1" by interpolation in its definition (as seen in Figure 4). With the temperature of PCM at the new instant, Eq.1 can be applied to determine the outlet temperature at the new instant, and so on.

If the system is in storage mode (Figure 3b) the PCM is not charged neither discharged by the air flux but it gains or losses energy depending on the outer climatic conditions. In this period, the power of heat exchange is calculated by Eq.5, where U is the outer thermal transmittance (1.13 $W/m^2 \cdot K$) and A_{out} (8.64 m^2)is the area of the outer skin.

$$\dot{Q}^n = U \cdot A_{out} \cdot \left(T_{PCM}{}^n - T_{ext}{}^n \right) \quad \text{(Eq.5)}$$

3. Results and discussion

The numerical methodologies previously described were compared against experimental data from the set-up located at Puigverd de Lleida (Spain). The experiments were based on the cold storage sequence, defined in Figure 3. Out of the experimental campaign carried out, here only the results from two days are presented (June 15th and July 22nd 2014) in order to evaluate the performance of the models under different weather conditions. Similarly as in the validation procedure presented in de Gracia et al. [18], the temperature of PCM is the parameter to validate in all the processes of the cold storage sequence (charge, storage and discharge), while outlet air temperature of the facade is also used for validation of the discharge process, since it is critical to quantify the thermal benefits of the system.

Figure 5 presents the comparison of the average PCM temperature between the numerical models and the experimental data during the charge processes driven in June. It can be seen that all the models predict the PCM temperature in a good agreement with the experiments during the charge process. The PCM temperature is slightly over predicted in all the models. Moreover, the effect of using measured inlet temperature or indoor/outdoor temperature as inlet can be noticed; however, this effect is not dominant and does not cause a significant error to the numerical models.

Furthermore, the performance of the different numerical methodologies during the discharge process is also compared against experimental data. On one hand, Figure 6 shows the evolution of the average PCM temperature during the discharge and on the other hand, the outlet air temperature is depicted in Figure 7. It is important to highlight that the outlet air temperature. In this case, it can be seen that the performance of the models is very similar and all of them slightly over-predict the PCM temperature.

The authors do not want to only provide a qualitatively experimental validation, as provided by the graphical comparison, but to provide a quantitative analysis of the deviations between the numerical predictions and the experimental data. Table 1 presents the absolute (Δx) and relative (δ) errors of all the studied numerical methodologies in the processes of charge, storage and discharge in comparison to the measured data in the set-up. According to the results shown in Table 1, it can be stated

that all the models can predict, with a high degree of accuracy, the average temperature of PCM during all the periods, presenting deviation to the experiments below 0.8ºC with a relative error smaller than 4% in all cases. Small differences were found between models in predicting the temperature of the PCM even though the isothermal model (IM) considers all the PCM to be at the same temperature, which indicates that this assumption is valid for the analysis of this system. Furthermore, important differences were observed when predicting the outlet temperature at the facade during the discharge process. In this case, the inlet boundary condition is critical, and using the source temperature (indoor/outdoor) increases significantly the error of the predicted value, as it can be seen when deviation from CV1 (around 1%) and CV2 (around 4%) are compared. The isothermal model, which also uses the source temperature as inlet, it presents a similar deviation to the experimental data (around 3%) than CV2 does. It is important to highlight that although the three models predict the outlet temperature with an absolute error below 1ºC, this error could lead to important deviations in the calculation of the discharge power, since it is calculated based on the temperature difference between the inlet and outlet of the facade channel. This effect might be important in systems with low power of discharge (small thermal gradient between inlet and outlet), and be minimized in systems with high heat transfer rates.

4. Conclusions

In order to include PCM in engineering and architectural designs, user-friendly tools are required to assist design processes of any industrial or building system. Numerical tools used to analyze the performance of these materials in different applications frequently require high level of specific knowledge and are developed for certain specific systems. This paper presents a simple methodology which can be used to predict the performance of LHTES systems without consuming high computational resources. In this case, the analyzed system is a ventilated double skin facade with PCM in its air chamber.

A simple isothermal model based on the assumption that all the PCM is at a single temperature is implemented in a non-iterative algorithm. Numerical results are compared against experimental data and a finite control volume numerical model. The validation process showed that the isothermal model, even presenting worse results than the finite control volume method, it can predict with a good accuracy the average

temperature of the PCM during the charge, storage and discharge processes, with deviations below 3%. Moreover, the outlet temperature was also predicted successfully using the simple isothermal model. The study also evaluated the effect of implementing indoor or outdoor air temperature as inlet temperature of the facade in the model. It was shown that this effect is not significant when predicting the PCM temperature but it affects the outlet temperature significantly.

It is important to highlight that the proposed methodology might be used for the incorporation of LTES systems in industrial processes or buildings, and evaluate its global performance, but not to design the LTES by itself, which might require more accurate and precise techniques.

The methodology presented in this paper could also be useful for other LHTES systems. The application of a similar approach to different PCM storage designs, as well as the evaluation of the most limiting hypothesis could shed light on this matter.

Nomenclature

A_{conv}	Area air-PCM heat transfer	[m^2]
A_{out}	Area heat losses	[m^2]
Cp	Heat capacity	[J g^{-1} K^{-1}]
h	Heat transfer coefficient	[W m^{-2} K^{-1}]
L	Enthalpy of fusion	[J g^{-1}]
$\dot{m}$	Air mass flow rate	[kg s^{-1}]
m_{PCM}	Mass of PCM	[kg]
$Q_{n \rightarrow n+1}$	Energy absorbed or released	[J]
$\dot{Q}^{n}$	Power of charge or discharge	[W]
U	Thermal transmittance	[W m^{-2} K^{-1}]
t	Time	[s]
T_{ext}	Outdoor temperature	[K]
T_{inlet}	Inlet temperature	[K]
T_{PCM}	Average PCM temperature	[K]
T_{outlet}	Outlet temperature	[K]

Greek symbols

Δx	Absolute error of variable “x”
δx	Relative error of variable “x”

Acknowledgements

The work partially funded by the Spanish government (ENE2011-28269-C03-01, ENE2011-22722 and ULLE10-4E-1305). The authors would like to thank the Catalan Government for the quality accreditation given to their research group (2014 SGR 123). The research leading to these results has received funding from the European Union's Seventh Framework Programme (FP7/2007-2013) under grant agreement n° PIRSES-GA-2013-610692 (INNOSTORAGE).

References

[1] Directive 2010/31/EU of the European parliament and of the council of 19 May 2010 on the energy performance of buildings. Available from: http://www.epbd-ca.eu

[2] International Energy Agency. Energy Technology Perspectives 2012. Pathways to a Clean Energy System. France, 2012.

[3] L.F. Cabeza, Thermal Energy Storage. In: Sayigh A, (ed.) Comprehensive Renewable Energy, Oxford: Elsevier, Vol 3, p. 211-253, 2012.

[4] I. Dincer, M.A. Rosen, Thermal energy storage (TES) methods. In: Dincer I and Rosen MA (eds.) Thermal Energy Storage: Systems and Applications, New York, NY: John Wiley & Sons, p. 93-212, 2002.

[5] V. Basecq, G. Michaux, C. Inard, P. Blondeau, Short-term storage systems of thermal energy for buildings: a review, Advances in Building Energy Research 7 (2013) 66-119.

[6] M. Pomianowsky, P. Heiselberg, Y. Zhang, Review of thermal energy storage technologies based on PCM application in buildings, Energy and Buildings 67 (2013) 56-69.

[7] E. Osterman, V.V. Tyagi, V. Butala, N.A. Rahim, U. Stritih, Review of PCM based cooling technologies for buildings, Energy and Buildings 49 (2012) 37-49.

[8] R. Foran, M.Wu, The capabilities and barriers of incorporating phase change material into residential building design in Sydney, Australia, International Journal of Engineering Practical Research, vol 2 Issue 4 (2013) 170-173.

[9] T. Silva, R. Vicente, N. Soares, V. Ferrerira, Experimental testing and numerical modelling of masonry Wall solution with PCM incorporation: A passive construction solution, Energy and Buildings 49 (2012) 235-245.

[10] N.A. Yahay, H. Ahmad, Numerical investigation of indoor air temperatura with the application of PCM gypsum board as ceiling panels in buildings, Procedia Engineering 20 (2011) 238-248.

[11] P. Dolado, A. Lazaro, J.M. Marin, B. Zalba, Characterization of melting and solidification in a real scale PCM-air heat exchanger: Numerical model and experimental validation, Energy conversion and management 52 (2011) 1890-1907.

[12] X. Jin, X. Zhang, Thermal analysis of a double layer phase change material floor, Applied Thermal Engineering 31 (2011) 1576-1581.

[13] A. de Gracia, L. Navarro, A. Castell, A. Ruiz-Pardo, S. Álvarez, L.F. Cabeza, Experimental study of a ventilated facade with PCM during Winter period, Energy and Buildings 58 (2013) 324-332.

[14] A. de Gracia, L. Navarro, A. Castell, A. Ruiz-Pardo, S. Álvarez, L.F. Cabeza, Thermal analysis of a ventilated facade with PCM for cooling applications, Energy and Buildings 65 (2013) 508-515.

[15] Rubitherm Technologies GmbH www.rubitherm.de

[16] D. Saelens, S. Roels, H. Hens, The inlet temperature as a boundary condition for multiple-skin facade modelling, Energy and Buildings 36 (2004) 825–835.

[17] S. Patankar, Numerical Heat Transfer, Hemisphere Publications, 1980.

[18] A. de Gracia, L. Navarro, A. Castell, L.F. Cabeza, Numerical study on the thermal performance of a ventilated facade with PCM, Applied Thermal Engineering 61 (2013) 372-380.

[19] P. Lamberg, R. Lehtiniemi, A.M.Henell, Numerical and experimental investigation of melting and freezing processes in phase change material storage, International Journal of Thermal Science 43 (2004) 277-287.

[20] M.M. Farid, A new approach in the calculation of heat transfer with phase change, 9th International Congress on Energy and Environment, Miami, 1989. p. 1-19.

[21] A. Bejan, A.D. Kreaus, Heat transfer handbook. John Wiley & Sons, Inc. United States of America 2003.

[22] Y.A. Çengel, Heat transfer. A practical approach. McGraw-Hill, Inc. United States of America, 1998.

Figure captions

Figure 1. Experimental set-up. Prototype of the VDSF with PCM

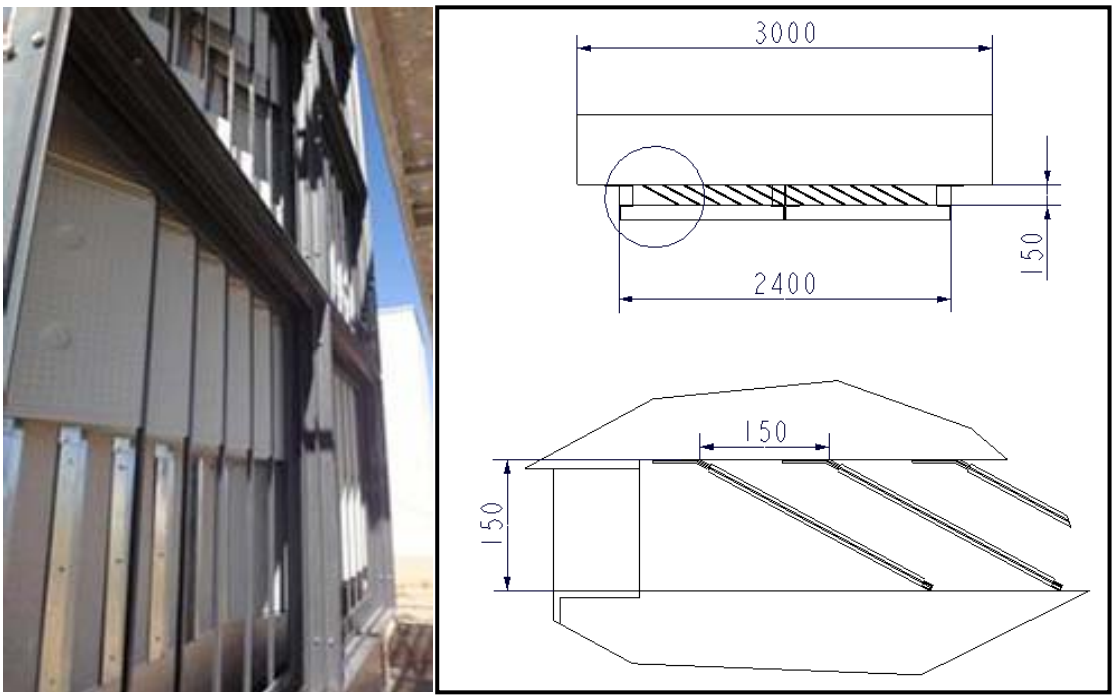

Figure 2. PCM panels distribution inside the air cavity of the VDSF

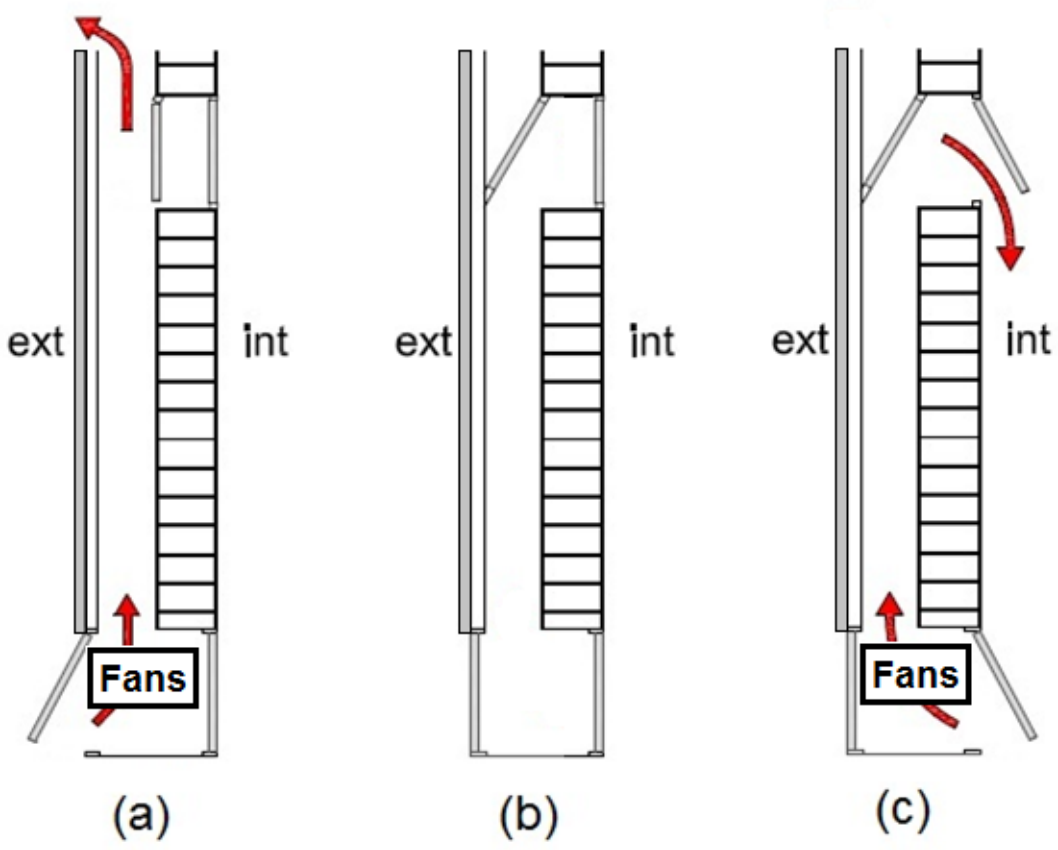

Figure 3. Operational schedule of the VDSF during summer period

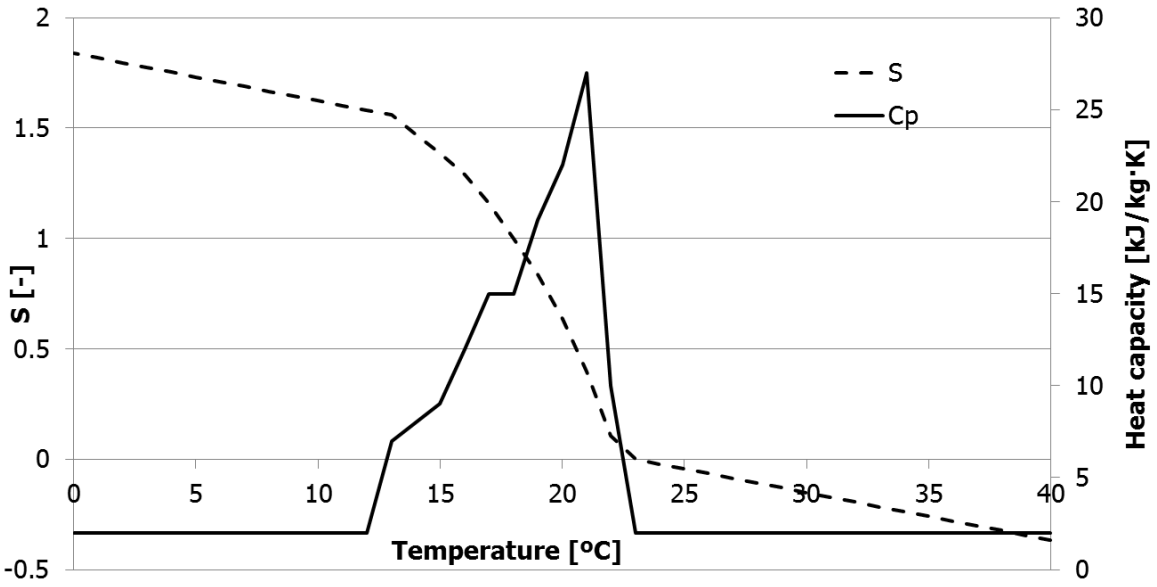

Figure 4. Heat capacity and S value in function of temperature

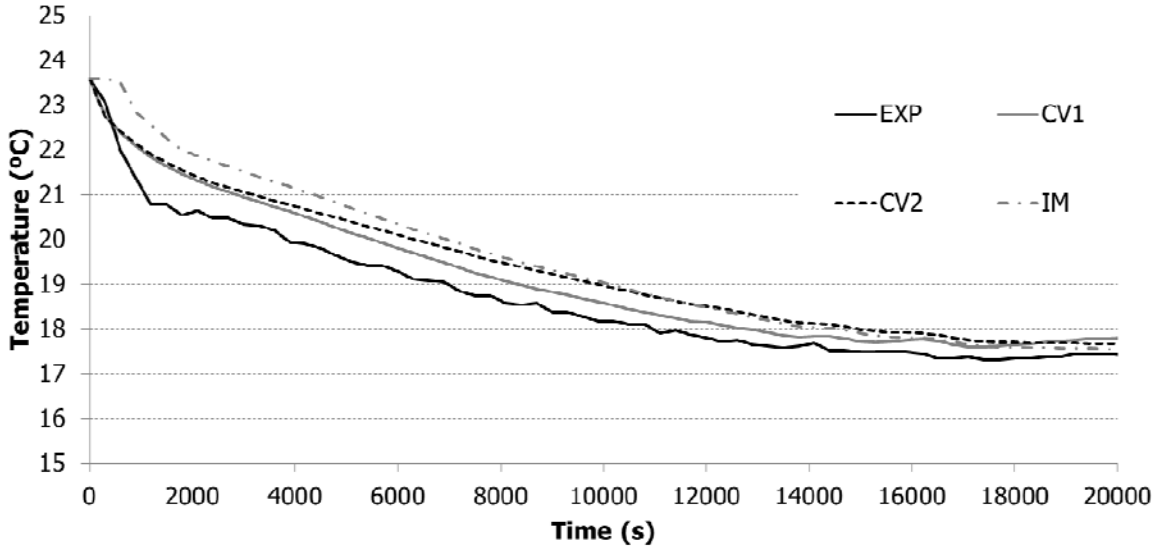

Figure 5. Comparison of average PCM temperature between numerical and experimental data. Charge process.

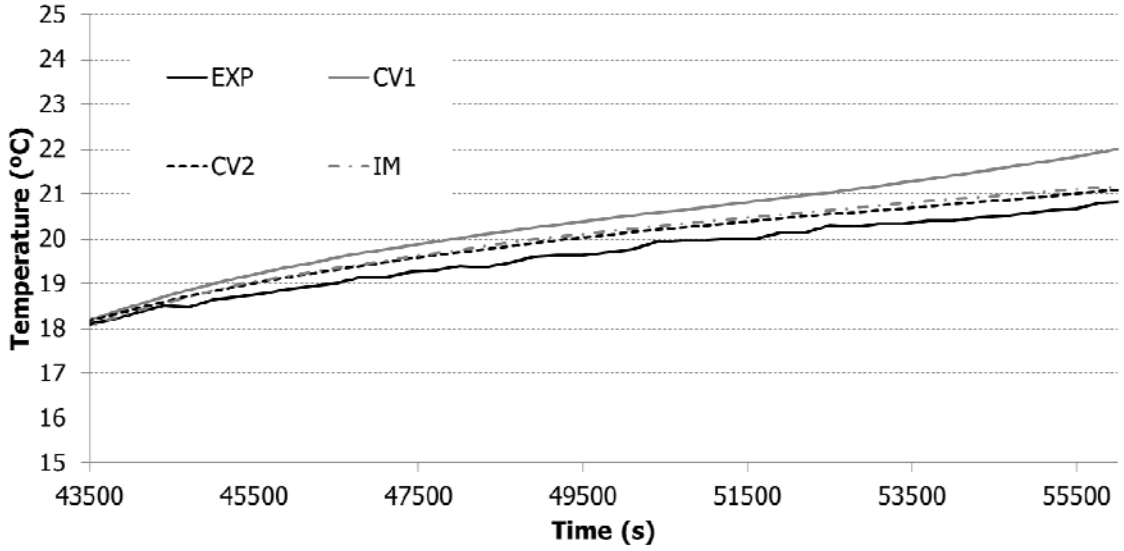

Figure 6. Comparison of average PCM temperature between numerical and experimental data. Discharge process.

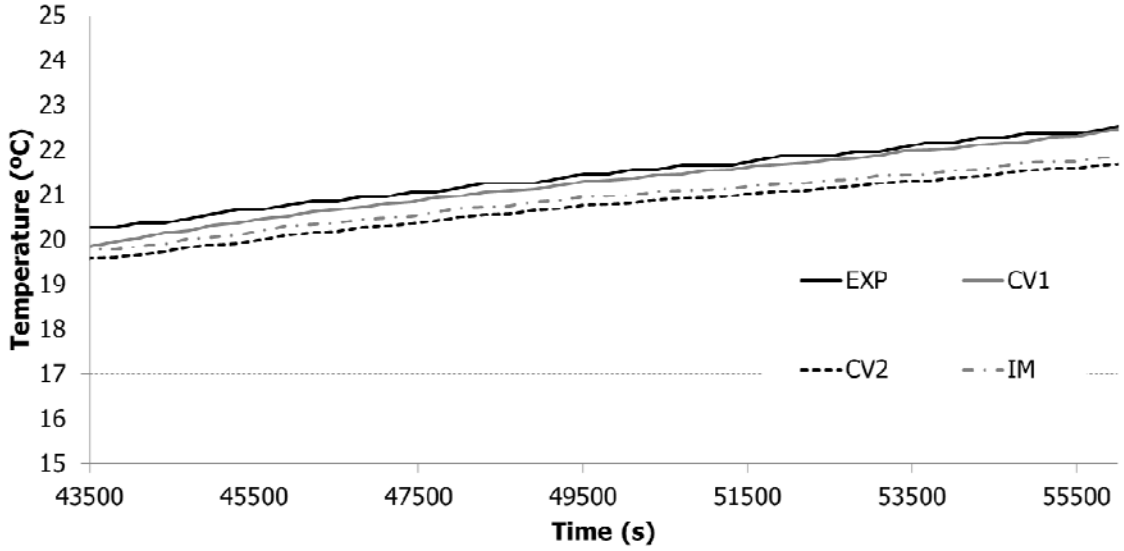

Figure 7. Comparison of outlet air temperature between numerical and experimental data. Discharge process.

Table 1. Absolute and relative error of the numerical prediction in comparison to the experimental data in the charge, storage and discharge processes.

		CHARGE		
		CV1	CV2	IM
Exp1 (June)	$\Delta_{T\ PCM}$ [ºC]	0.43	0.54	0.55
	$\delta_{T\ PCM}$ (%)	2.29	2.84	2.82
Exp 2 (July)	$\Delta_{T\ PCM}$ [ºC]	0.25	0.14	0.33
	$\delta_{T\ PCM}$ (%)	1.28	0.66	1.70

		STORAGE		
		CV1	CV2	IM
Exp1 (June)	$\Delta_{T\ PCM}$ [ºC]	0.40	0.37	0.04
	$\delta_{T\ PCM}$ (%)	2.21	2.09	0.21
Exp 2 (July)	$\Delta_{T\ PCM}$ [ºC]	0.23	0.21	0.30
	$\delta_{T\ PCM}$ (%)	1.30	1.16	1.66

		DISCHARGE		
		CV1	CV2	IM
Exp1 (June)	$\Delta_{T\ PCM}$ [ºC]	0.76	0.30	0.35
	$\delta_{T\ PCM}$ (%)	3.61	1.43	1.68
	$\Delta_{T\ out}$ [ºC]	0.20	0.76	0.55
	$\delta_{T\ out}$ (%)	1.03	3.85	2.78
Exp 2 (July)	$\Delta_{T\ PCM}$ [ºC]	0.19	0.20	0.39
	$\delta_{T\ PCM}$ (%)	0.82	2.34	3.53
	$\Delta_{T\ out}$ [ºC]	0.17	0.95	0.70
	$\delta_{T\ out}$ (%)	0.86	4.33	3.19